Micro- and nanoelectronics. Condensed matter physics

Микро- и наноэлектроника. Физика конденсированного состояния

UDC 532.6, 53.06, 535.016
https://doi.org/10.32362/2500-316X-2024-12-5-50-62
EDN LYYDJX

CC BY

RESEARCH ARTICLE

Effect of surface electromagnetic wave treatment on the refractive properties of thin films based on indium tin oxides with laser-deposited single-walled carbon nanotubes

Andrei S. Toikka [1, 2, @], Natalia V. Kamanina [1, 2, 3, 4]

[1] *St. Petersburg Electrotechnical University, St. Petersburg, 197022 Russia*
[2] *Petersburg Nuclear Physics Institute, National Research Center "Kurchatov institute", Gatchina, 188300 Russia*
[3] *Scientific and Production Corporation "S.I. Vavilov State Optical Institute", St. Petersburg, 192171 Russia*
[4] *Vavilov State Optical Institute, St. Petersburg, 199053 Russia*
[@] *Corresponding author, e-mail: astoikka.nano@gmail.com*

Abstract

Objectives. The article investigates the effect of surface electromagnetic wave (SEW) treatment on the refractive properties of thin conducting films based on indium tin oxide (ITO) with laser-deposited single-walled carbon nanotubes (CNTs). The effective thickness of the layer of laser-deposited CNTs before and after SEW treatment is evaluated.

Methods. A laser-oriented deposition method employing a CO_2 laser (λ = 10.6 μm) was used to form the structures. Diagnostics of modifications of ITO thin films were carried out using an ellipsometer operating in the spectral range of 300–1000 nm. The Cauchy model was used to describe the optical properties of K8 crown substrates and ITO thin films. To interpret the ellipsometry results of ITO modifications with CNTs, an effective-thickness virtual layer model was introduced. During post-processing of the surface, a CO_2 marker (λ = 10.6 μm) was used to generate SEW. The influence of SEW treatment on the thickness of the virtual layer was assessed using ellipsometry and atomic force microscopy in contact mode.

Results. Based on the ellipsometry data, the effective thickness of the CNT layer was in the range of 24–26 nm. Following SEW treatment, the thickness of the effective CNT layer decreased to 4–8 nm, indicating the possibility of precision processing of the ITO surface with CNTs using SEW. When CNTs are deposited on an ITO surface with subsequent SEW treatment of the surface, reflection losses for p-polarized radiation are reduced. In a spectral range of 400–750 nm at an angle of incidence relative to the normal to the plane of structures α = 65°, a decrease in reflection is observed from 18.5% to 13.5% relative to ITO without CNTs and SEV treatment; at α = 71°, a decrease from 6.4% to 4.7% is observed; at α = 77°, a decrease from 1.8% to 1.2%.

Conclusions. For ITO-based thin films with laser-deposited CNTs, the described SEW treatment method provides a precise reduction in the thickness of the composite structure while preserving the antireflective properties of the CNTs. These capabilities make it possible to use the studied ITO modifications in solving problems in optical electronics, microfluidics, and biomedicine.

Keywords: indium tin oxides, carbon nanotubes, laser exposure, surface electromagnetic wave treatment

© A.S. Toikka, N.V. Kamanina, 2024

• **Submitted:** 05.02.2024 • **Revised:** 14.03.2024 • **Accepted:** 12.07.2024

For citation: Toikka A.S., Kamanina N.V. Effect of surface electromagnetic wave treatment on the refractive properties of thin films based on indium tin oxides with laser-deposited single-walled carbon nanotubes. *Russ. Technol. J.* 2024;12(5):50–62. https://doi.org/10.32362/2500-316X-2024-12-5-50-62

Financial disclosure: The authors have no financial or property interest in any material or method mentioned.

The authors declare no conflicts of interest.

НАУЧНАЯ СТАТЬЯ

Влияние обработки поверхностными электромагнитными волнами на рефрактивные свойства тонких пленок на основе оксидов индия и олова с лазерно-осажденными одностенными углеродными нанотрубками

А.С. Тойкка [1, 2, @], **Н.В. Каманина** [1, 2, 3, 4]

[1] *Санкт-Петербургский государственный электротехнический университет «ЛЭТИ», Санкт-Петербург, 197022 Россия*
[2] *НИЦ Курчатовский институт – Петербургский институт ядерной физики «ПИЯФ», Гатчина, 188300 Россия*
[3] *НПО ГОИ им. С.И. Вавилова, Санкт-Петербург, 192171 Россия*
[4] *ГОИ им. С.И. Вавилова, Санкт-Петербург, 199053 Россия*
[@] *Автор для переписки, e-mail: astoikka.nano@gmail.com*

Резюме

Цели. Цель работы – исследование влияния обработки поверхностными электромагнитными волнами (ПЭВ) тонких проводящих пленок на основе оксидов индия и олова (indium tin oxides, ITO) с лазерно-осажденными одностенными углеродными нанотрубками (УНТ) на рефрактивные свойства, оценка эффективной толщины слоя лазерно-осажденных УНТ до и после ПЭВ-обработки.

Методы. Для формирования структур использовался метод лазерно-ориентированного осаждения с применением CO_2-лазера (λ = 10.6 мкм). Диагностика модификаций тонких пленок ITO осуществлялась при помощи эллипсометра в спектральном диапазоне 300–1000 нм. Для описания оптических свойств подложек крон К8 и тонких пленок ITO использовалась модель Коши. Для интерпретации результатов эллипсометрии модификаций ITO с УНТ была введена модель виртуального слоя с эффективной толщиной. При постобработке поверхности использовался CO_2-маркер (λ = 10.6 мкм) для генерации ПЭВ. Оценка влияния ПЭВ-обработки на толщину виртуального слоя проводилась при помощи эллипсометрии и атомно-силовой микроскопии в контактном режиме.

Результаты. На основе данных эллипсометрии установлено, что эффективная толщина слоя УНТ находилась в диапазоне 24–26 нм. После ПЭВ-обработки толщина эффективного слоя УНТ снизилась до 4–8 нм. При осаждении УНТ на поверхность ITO и последующей ПЭВ-обработке поверхности снижаются потери на отражение для p-поляризованного излучения. В спектральном диапазоне 400–750 нм при угле падения относительно нормали к плоскости структур 65° наблюдается снижение отражения с 18.5% до 13.5% относительно ITO без УНТ и ПЭВ-обработки, при 71° – снижение с 6.4% до 4.7%, при 77° – снижение с 1.8% до 1.2%.

Выводы. Для тонких пленок на основе ITO с лазерно-осажденными УНТ доступен метод ПЭВ-обработки, которая позволяет сохранить просветляющие свойства УНТ и обеспечивает прецизионное снижение толщины композитной структуры. Указанные возможности позволяют использовать исследуемые модификации ITO в задачах оптической электроники, микрофлюидики и биомедицины.

Ключевые слова: оксиды индия и олова, углеродные нанотрубки, лазерное воздействие, обработка поверхностными электромагнитными волнами

• **Поступила:** 05.02.2024 • **Доработана:** 14.03.2024 • **Принята к опубликованию:** 12.07.2024

Для цитирования: Тойкка А.С., Каманина Н.В. Влияние обработки поверхностными электромагнитными волнами на рефрактивные свойства тонких пленок на основе оксидов индия и олова с лазерно-осажденными одностенными углеродными нанотрубками. *Russ. Technol. J.* 2024;12(5):50–62. https://doi.org/10.32362/2500-316X-2024-12-5-50-62

Прозрачность финансовой деятельности: Авторы не имеют финансовой заинтересованности в представленных материалах или методах.

Авторы заявляют об отсутствии конфликта интересов.

INTRODUCTION

Indium tin oxides (ITO) are degenerate semiconductors with *n*-type conductivity [1–3]. Their properties depend largely on the stoichiometric composition $(In_2O_3)_x$–$(SnO_2)_{1-x}$. Here, SnO_2 is used to increase electron concentration (N). It has been shown [1] that, in a pure In_2O_3 matrix ($x = 0$), electron concentration $n_e = 1 \cdot 10^{20}$ cm^{-3}. In the range $0.02 < x < 0.15$, the N value increases up to $9 \cdot 10^{20}$ cm^{-3}. Further increase of SnO_2 content is not reasonable due to the decreased mobility of charge carriers μ [1].

The criterion for comparing the parameters of ITO films depends on the application. When considering ITO as electrical contacts, it is necessary to minimize the resistivity ρ. In the case of ITO, the value of this parameter varies in the range of 10^{-4}–10^{-3} Ohm·cm [1–3]. In addition to varying the stoichiometric composition of ITO, the electrical properties optimized by altering the heating rate of substrates during deposition [2], selecting the types of working gases and their partial pressures [3–5], and using different targets [6].

In some cases, for example, in photovoltaics [7] and liquid crystal optics [8], high optical transmittance is required in addition to low electrical resistivity. In the visible and near-infrared (near-IR) spectral regions, this requirement is fulfilled due to the relatively low extinction coefficient k of ITO in this range; thus, optical losses are mainly due to reflection [9].

Indium and tin oxides also represent sought-after structures in IR optics due to the presence of plasmonic electron gas resonance in this range. Here, the plasma frequency ω_{pl} and damping frequency γ depend on the concentration and mobility of charge carriers, respectively [10]. By varying the above parameters, it is possible to obtain spectral regions with a negative value of dielectric permittivity, which finds a number of applications, e.g., in modulators [11], solar cells [12], and sensors [13].

Thus, ITO applications are largely determined by the concentration and mobility of electrons. One of the strategies to improve the ITO performance is the use of composite materials with nanostructures, by which means it is possible to reduce the electrical resistance and tune the restricted bandgap width [14–16].

Significant results were achieved by laser-oriented deposition of carbon nanotubes on the ITO surface [17–19]. Carbon nanotubes (CNTs) have been shown to contribute to an increase in optical transmittance, improved mechanical and laser strength, and reduced electrical resistance of ITO thin films. Based on atomic force microscopy data [19], CNTs are understood to be deposited in the form of clusters.

In order to model the developed electro-optical devices, in which one of the key elements is a structured ITO layer, it is necessary to take into account the basic properties of the CNT layer, including its thickness. Since this material is not deposited as a continuous layer, there is a need for a separate study devoted to the determination of the CNT layer thickness. In the present work, approach nondestructive ellipsometry was chosen as the diagnostic method due to the possibility of examining relatively large apertures. The current study also investigated the precision variation of CNT layer thickness. Surface electromagnetic wave (SEW) treatment was selected as the mechanism for providing thickness modification.

1. MATERIALS AND METHODS

The formation of ITO thin films on K8 crown glass substrates (Scientific and Production Corporation S.I. Vavilov State Optical Institute, Russia) was carried out by laser-oriented deposition [17] using a CO_2 laser (Laser Center, Russia; wavelength $\lambda = 10.6$ μm;

power $P \approx 30$ W; beam diameter $d = 5$ mm). Cerac, Inc. (USA) provided ITO pellets with stoichiometric composition $(In_2O_3)_{0.9}$–$(SnO_2)_{0.1}$. The average thickness of the considered ITO films was 80–100 nm with mean-square roughness *Sq* less than 2 nm. Next, Aldrich (USA) brand single-walled carbon nanotubes (CNTs, No. 704121, chirality <7.6>) were deposited on a part of the samples with ITO films by laser-oriented deposition.) A control field with an average strength of 100 V/cm was used in the CNT deposition process. This is necessary to increase the kinetic energy of CNTs to provide their subsequent implantation on the material surface [17–19].

The thickness and roughness of the films were controlled using an atomic force microscope NT-MDT Solver Next (NT-MDT, Russia) in contact mode with a scanning frequency of 1 Hz. Refractive properties were investigated on a J.A. Woolam M-2000RCE ellipsometer (J.A. Woolam, USA) with built-in *CompleteEASE* software (version 4.91)[1]. For this purpose, the complex reflectance indices for s- and p-polarized radiation were r_p and r_s, respectively. Then, according to the ellipsometry equation (1), the ellipsometric parameters ψ and Δ were determined on the basis of the measured complex reflection indices $\dot{r}_p$ and $\dot{r}_s$ and phase difference in reflection from the interface δ_p and δ_s [20][2]:

$$\frac{\dot{r}_p}{\dot{r}_s} = \frac{|\dot{r}_p|}{|\dot{r}_s|} e^{j(\delta_p - \delta_s)} = \operatorname{tg}\psi e^{j\Delta}. \quad (1)$$

This expression is used in the Jones formalism; the parameters r_p and r_s correspond to the diagonal elements of the Jones matrix [20], which are valid for fully polarized radiation. In order to avoid unnecessary artifacts in the interpretation of ellipsometry results, the Stokes–Mueller formalism was used to take into account the degree *P* in the interaction of radiation with the studied samples [20]. In this approach, the Stokes matrices of the output and input radiation are related using the Mueller matrix $\mathbf{M}$[2]:

$$\mathbf{M} = R\begin{bmatrix} 1 & -PN & 0 & 0 \\ -PN & 1 & 0 & 0 \\ 0 & 0 & PC & PS \\ 0 & 0 & -PS & PC \end{bmatrix}. \quad (2)$$

Parameters *N*, *C*, *S* are related to the ellipsometric angle ψ and Δ[2]:

$$\begin{cases} N = \cos 2\psi, \\ C = \sin 2\psi \cos\Delta, \\ S = \sin 2\psi \sin\Delta. \end{cases} \quad (3)$$

The abovementioned parameters are normalized by reflection coefficient by intensity:

$$R = \frac{1}{2}(\dot{r}_s \dot{r}_s^* + \dot{r}_p \dot{r}_p^*) = \frac{R_s + R_p}{2}. \quad (4)$$

In expression (3), R_s and R_p correspond to the intensity reflection coefficients for s- and p-type polarization, respectively. When analyzing the spectral dependencies $\dot{r}_p$ and $\dot{r}_s$ along with their complex conjugate values $\dot{r}_p^*$ and $\dot{r}_s^*$, it is necessary to take into account the complex refractive indices $(\dot{n}_i)$ of the corresponding media [20]:

$$\begin{cases} \dot{n}_i = n_i + jk_i, \\ \dot{r}_p = \dfrac{\dot{n}_1 \cos\varphi_0 - \dot{n}_0 \cos\varphi_1}{\dot{n}_1 \cos\varphi_0 + \dot{n}_0 \cos\varphi_1} = |\dot{r}_p| e^{j\delta_p}, \\ \dot{r}_s = \dfrac{\dot{n}_1 \cos\varphi_0 - \dot{n}_1 \cos\varphi_1}{\dot{n}_1 \cos\varphi_0 + \dot{n}_1 \cos\varphi_1} = |\dot{r}_s| e^{j\delta_s}. \end{cases} \quad (5)$$

Parameter *n* is the refractive index of the medium, while *k* is the extinction coefficient. The radiation propagates in the medium with $i = 0$ and is reflected from the interface with $i = 1$, where *i* is the order number of the medium. Thus, the complex index of the studied structures is related to the amplitudes and phases of the complex reflection coefficients (4), which are measured using an ellipsometer. Using expression (1), the ellipsometric parameters ψ and Δ are determined to obtain the components of the Mueller matrix (2)–(3). In order to determine the refractive indices of K8 crown substrates, ITO thin films and their modifications, it is necessary to solve the inverse ellipsometry problem. This problem is reduced to the selection of those values of the parameters of refractive indices, extinction coefficients, and material thicknesses at which the values of *N, C, S* obtained with the help of the selected model will have the least divergence from the experimental data. For this purpose, we used the minimization of mean square error (*MSE*)[2]:

$$MSE = \sqrt{\frac{1}{3n-m}} \times \sqrt{\sum_{l=1}^{n}\left[(N_l^{\text{mod}} - N_l^{\text{exp}})^2 + (C_l^{\text{mod}} - C_l^{\text{exp}})^2 + (S_l^{\text{mod}} - S_l^{\text{exp}})^2\right]}. \quad (6)$$

[1] https://www.jawoollam.com/ellipsometry-software/completeease. Accessed April 21, 2024.

[2] *Complete EASE: Data Analysis Manual* (*version 4.63*). J.A. Wollam Co., Inc. 2011. 410 p.

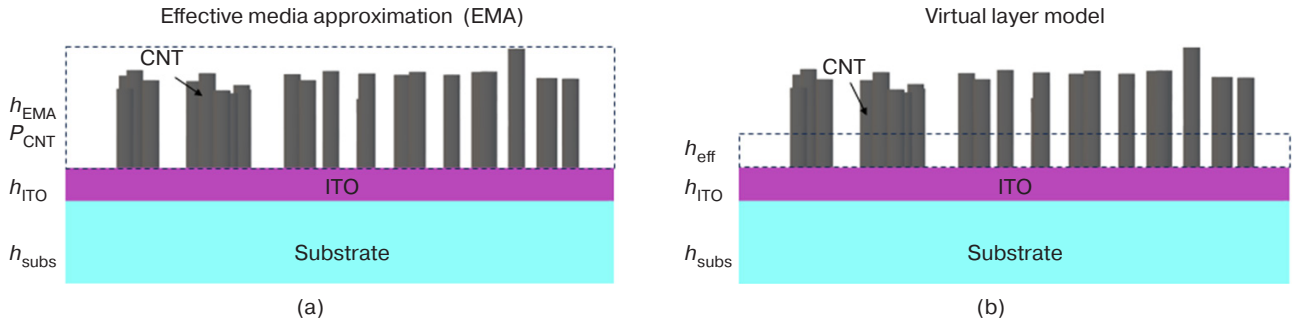

Fig. 1. Interpretation of layers based on CNT:
(a) solid medium model; (b) virtual layer model.
h_{ITO} is the thickness of the ITO, h_{subs} is the thickness of the substrate

Parameter n corresponds to the number of iterations (in the spectral range 300–1000 nm the sources on the ellipsometer have 710 wavelength iterations), m is the number of fitting parameters. For the characterization of K8 crown substrates it is necessary to know the refractive index and extinction dependencies, as well as the roughness ($m = 3$). For ITO modifications, in addition to the above parameters, the thickness is also unknown ($m = 4$). Index l is the iteration number, *mod* and *exp* denote data based on approximation (model) and experiment, respectively.

The Cauchy model [21] was chosen to approximate the refractive index of K8 and ITO crown substrates in the spectral range of 300–1000 nm:

$$n(\lambda) = A + \frac{B}{\lambda^2} + \frac{C}{\lambda^4}. \quad (7)$$

This model describes the refractive index of ITO in the selected range with a high degree of confidence [22].

When CNT are deposited on the ITO surface, it is necessary to take into account the fact that these nanoparticles are deposited in clusters rather than as continuous layers [19]. However, to interpret the results, a value of the CNT layer thickness is necessary. For this purpose, we introduce the value of the effective thickness h_{eff} of the CNT layer according to the following assumptions:

1. Effective thickness parameter h_{eff} increases with increasing deposition density and with decreasing distance between deposited CNT clusters;
2. The extinction $k = f(\lambda)$ and refractive index $n = f(\lambda)$ of this layer are fixed and do not depend on the treatment;
3. Optical properties at the 'virtual layer–ITO' interface change discontinuously.

The abovementioned approach can be compared with Bruggemann's effective medium approximation (EMA), in which the layer thickness h_{EMA} is fixed and the variable parameter is the percentage content of components; in particular, component 1 is air, while component 2 is the material [20]. In the effective thickness approximation, the component content is taken as 100% ($P_{CNT} = 1$), while the varying parameter is the effective thickness h_{eff}. A visual comparison of the approaches is presented in Fig. 1.

Results of [23] were used as reference data for the description of n and k CNT. Interpretation of the results of ellipsometry of CNT/ITO/K8 crown structures was performed after determining the fitting parameters of K8 crown and ITO/K8 crown structures. When working with the CNT layer, the virtual layer model was used. The refractive index and extinction coefficients in the range of 300–1000 nm were imported from the data [23], while the fitting parameter was the thickness of the effective layer.

After diagnosing the structures based on ITO with CNTs, a part of the samples was subjected to laser treatment at CO_2 marker (λ = 10.6 μm, modulation frequency 1 kHz, beam diameter 150 μm, processing frequency 50 mm/s, power 21 W).

2. RESULTS AND DISCUSSION

According to the previously described procedures, the spectral dependencies of the refractive index of K8 crown substrates and ITO thin films deposited on K8 crown substrates were sequentially determined (Fig. 2). In the spectral range of 300–1000 nm, the Cauchy fitting parameters for the K8 crown substrates were as follows: $A = 1.550$, $B = 0.00541$ and $C = -9.153 \cdot 10^{-7}$ (Fig. 2a). The parameters for the ITO thin films were as follows: $A = 1.506$, $B = 0.085$ and $C = -3.72 \cdot 10^{-8}$ (Fig. 2b). From Fig. 2a, it can be concluded that the refractive index dispersion is negative; in the visible range, the refractive index varies between 1.51 and 1.54, which is typical for crown glasses[3]. Here, the optical parameters of ITO depend on the stoichiometric composition, deposition methods and modes, as well as the annealing temperature and post-processing procedures. In spite of this, the data

[3] GLASS—glasses, Refractive index database. https://refractiveindex.info/. Accessed April 21, 2024.

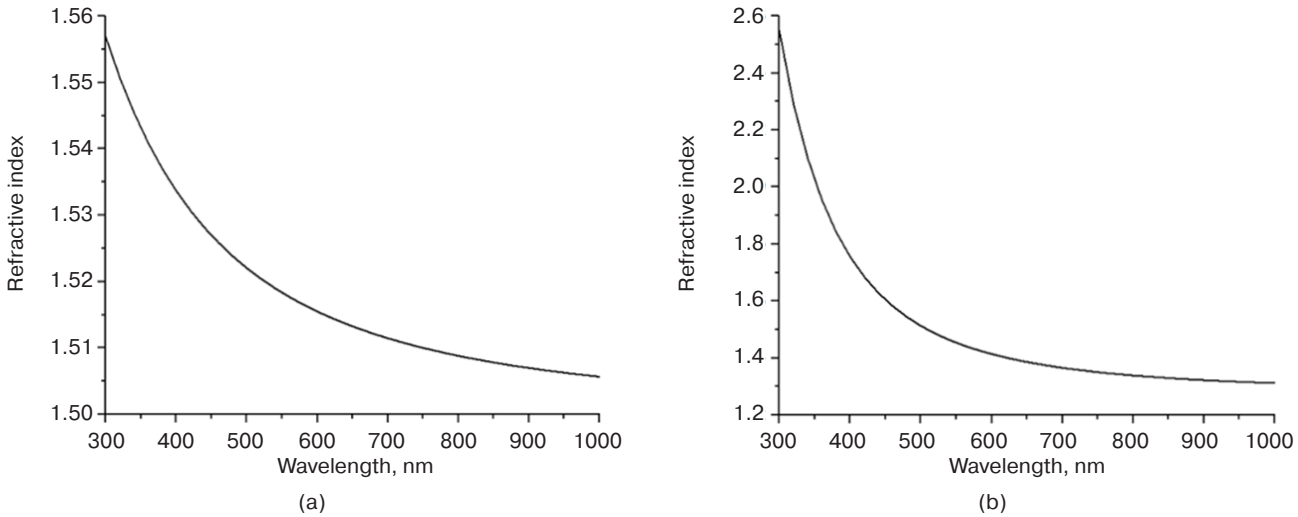

Fig. 2. Spectral dependencies of the refractive index: (a) K8 crown substrates, (b) ITO thin films

in Fig. 2b can be qualitatively compared with the results obtained in [22] to obtain a close correspondence.

The studied ITO structures are thin-film structures as manifested in the form of interference extrema (Fig. 3). The spectral dependencies were measured at three angles of incidence value (α = 65°, 71°, and 77°), which exceed the Brewster angle θ_{Br}. In the case of ITO, the value of θ_{Br} in the visible spectral range varies between 60.6° and 64.1°. Such a choice of incidence angles allows us to work with a steep section of the $R_p = f(\alpha)$ dependence, to reduce the noise/reflected signal ratio, and thus to interpret the ellipsometry results more reliably.

The data in Fig. 3 illustrate only the amplitude values of reflection coefficients, which are used to compare structures in the context of their application. To determine the thickness of ITO films by the optical method, we use the ellipsometric parameters ψ and Δ (Fig. 4), then follow the procedures described in step 1.

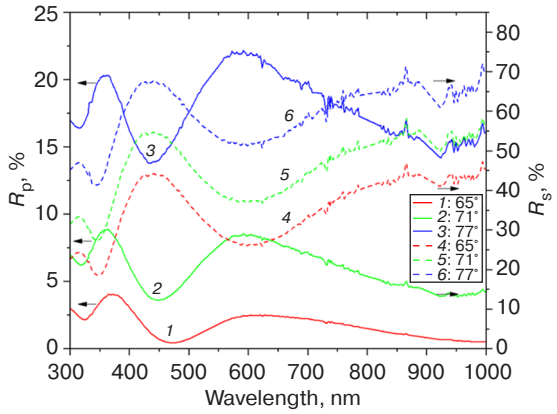

Fig. 3. Spectral dependencies of reflection coefficients of ITO thin films on glass in the range of 300–1000 nm at different angles of incidence: 65°, 71°, and 77°

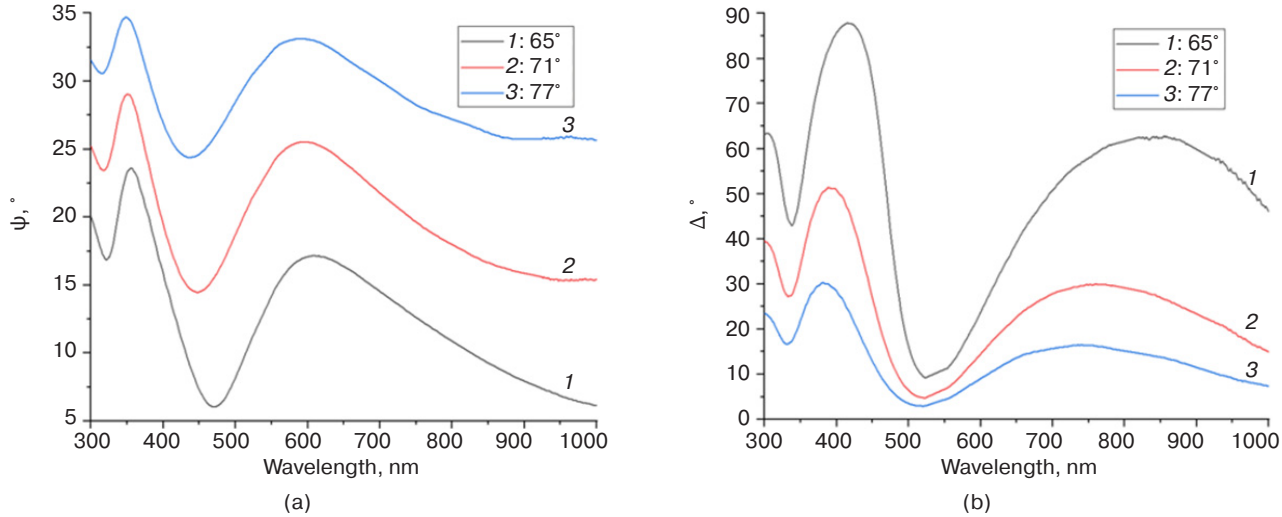

Fig. 4. Spectral dependencies of ellipsometric parameters ψ (a) and Δ (b) of ITO films on K8 crown substrate in the range of 300–1000 nm at different angles of incidence: 65°, 71°, and 77°

Based on the measured dependencies of reflection coefficients (Fig. 3), calculated ellipsometric parameters (Fig. 4), and known refractive properties (Fig. 2), it was found that the minimum *MSE* corresponds to an ITO thickness equal to 87 nm.

During CNT deposition, the number of extrema in the spectral dependencies of reflectance coefficients increases (Fig. 5), which is associated with an increase in optical length.

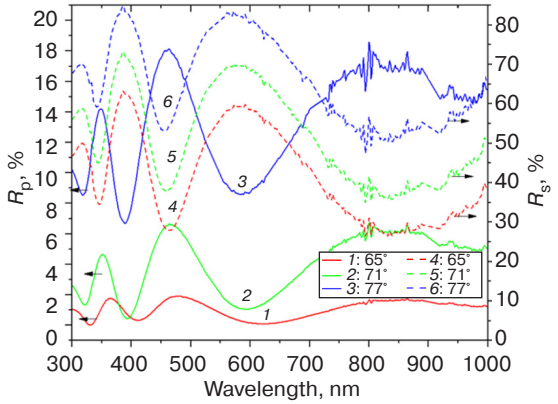

Fig. 5. Spectral dependencies of reflection coefficients of ITO thin films with laser-deposited CNTs on the K8 crown substrate in the range of 300–1000 nm at different angles of incidence: 65°, 71°, and 77°

It is noteworthy that the value of the reflection coefficient decreases during CNT deposition. For example, the values of local maxima of R_p at α = 65° in the case of ITO were 20.3% (λ = 358.3 nm) and 22.0% (λ = 591.4 nm), and 14.2% (λ = 348.5 nm) and 18.1% (λ = 463.3 nm) in the case of ITO with CNT. A more detailed comparison is given in the table.

In order to define the effective thickness of the CNT layer, it is necessary to take the ellipsometric parameters into account (Fig. 6). Then, also considering the thickness of the ITO layer (87 nm) calculated at the previous step, the procedure is performed as described in step 1. In this case, the minimum *MSE* corresponds to the effective thickness of the CNT layer in a range of 22–24 nm.

The effective thickness of the CNT layer depends on the density of cluster deposition and their sizes, which are determined by the mode of their deposition on the ITO surface. The required effect of the CNT layer on the ITO surface can involve the rearrangement of spectral properties, the formation of an orienting effect or a change in the free surface energy [17, 24]. As a rule, several parameters are changed at once, for example, surface energy and transmittance (including due to interference and formation of charge transfer complexes). Sometimes the reverse procedure is required, i.e., reducing the thickness of thin films, for example, based on the requirements for optical coordination of functional layers of optoelectronic devices.

In some cases, it becomes possible to treat the ITO surface via SEW [25]. In this treatment method, the SEW is distributed along the interface between the ITO surface and air. If we denote the dielectric permittivity of the ITO modification as ε_2 and of the boundary layer (air) as ε_1, the depth of the SEW attenuation l_2 in ITO can be estimated as follows [25]:

$$l_2 = \frac{c}{\omega}\sqrt{-\frac{(\varepsilon_1+\varepsilon_2)}{\varepsilon_2^2}}. \quad (8)$$

Here c and ω are the velocity of propagation in vacuum and frequency of radiation of electromagnetic waves, respectively. This approach imposes requirements on the dielectric permittivity of the treated material: $|\varepsilon_2| > \varepsilon_1$ and $\varepsilon_2 < 0$. The possibility of satisfying this

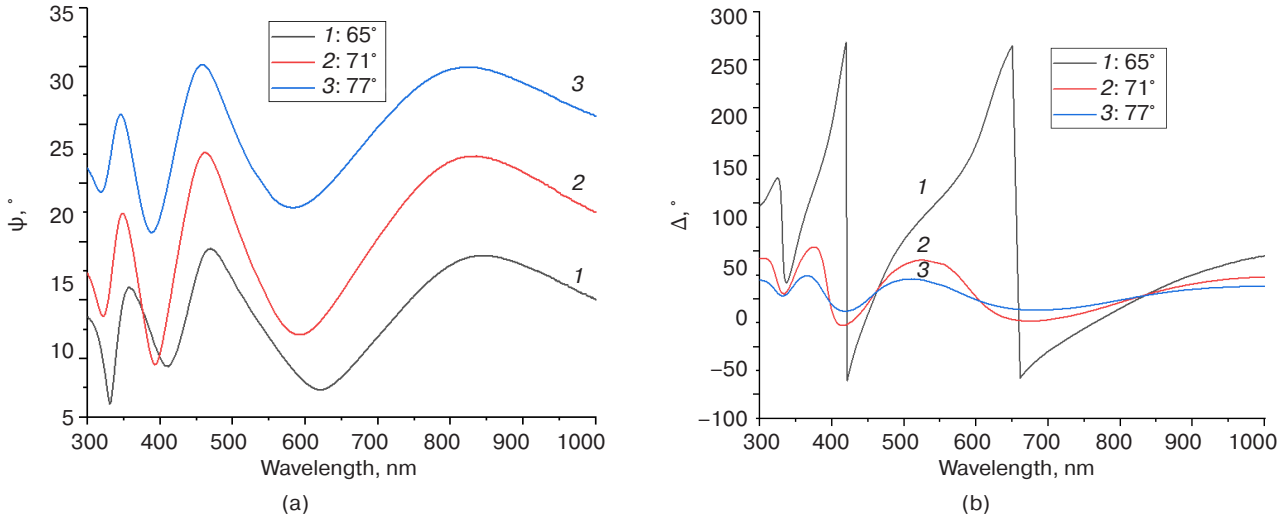

Fig. 6. Spectral dependencies of ellipsometric parameters ψ (a) and Δ (b) of ITO films with CNTs on K8 crown substrate in the range of 300–1000 nm at different angles of incidence: 65°, 71°, and 77°

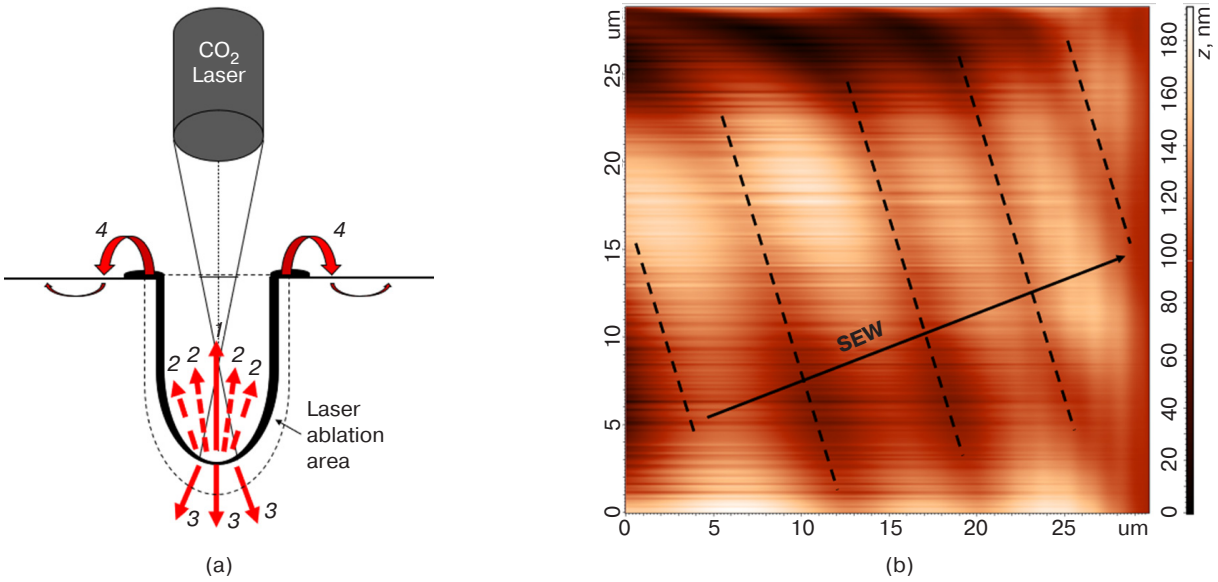

Fig. 7. SEW treatment:
(a) treatment scheme: *1* mirror-reflected flux, *2* diffuse-reflected flux, *3* refracted radiation flux, *4* SEW;
(b) atomic force microscopy profile of ITO surface in the area of SEW treatment

condition near the resonant frequencies ω_{pl} was already discussed in the introduction section.

SEW treatment should be distinguished from laser ablation by direct hit of radiation. The input radiation from the CO_2 laser was used to generate SEW, a significant part of which was absorbed by the ITO-based thin film with the formation of caverns, while a small part was diffusely reflected. Consequently, the SEW treatment exposed regions **around** the direct laser ablation zones, with energy densities for SEW exposure substantially lower than those required for laser ablation activation. The schematic differences are shown in Fig. 7 along with the surface profile of ITO modifications following SEW treatment.

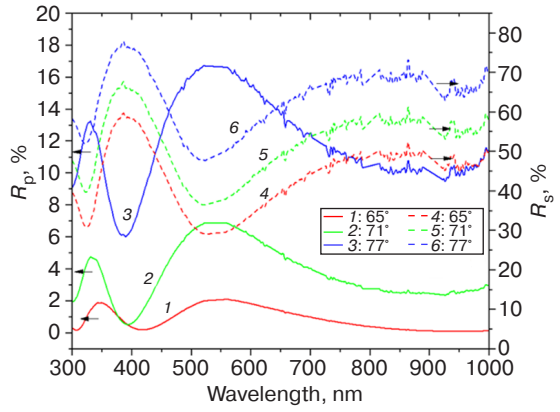

Fig. 8. Spectral dependencies of reflection coefficients of ITO thin films with laser-deposited CNT on the K8 crown substrate after SEW treatment in the range of 300–1000 nm at different angles of incidence: 65°, 71°, and 77°

The spectral dependencies of the surface reflectance coefficients of ITO thin films with CNT in the SEW treatment regions are shown in Fig. 8.

According to the position of the interference peaks, the optical length it can be seen to have decreased relative to the ITO films with CNT. At the same time, the numerical values of reflection coefficients are lower than in the case of the original ITO. The comparative data are presented in the table.

Spectral dependencies of ellipsometric parameters (Fig. 9) were also used to estimate the effective CNT layer thickness after SEW treatment, followed by the statistical processing described in step 1.

Based on the data shown in Figs. 8 and 9, it can be stated that the minimum *MSE* corresponds to $h_{eff} \approx 6$ nm. Similar procedures were carried out for 10 regions of ITO/CNT and ITO/CNT/SEW structures. It was found that h_{eff} decreases from 22–24 nm to 4–8 nm during the SEW treatment (Fig. 10).

At first glance (Fig. 10), there is some doubt about the presence of CNT after SEW treatment. On a macro-scale, the markers of CNT represent the reduced reflection loss (related to the luminescent effect of CNT with respect to ITO) and the increased contact wetting angle (related to the formation of Wenzel and Cassie–Baxter states on the CNT framework) [19, 24]. The comparison of reflection losses given earlier can be visualized in the table. A detailed analysis of the wetting mechanisms of the original structures was considered separately in [19]. ITO surfaces with CNT and SEW treatment preferentially possess contact angles θ in the range of 100° to 110°, while this range is 80°–90° for ITO surfaces with SEW, and 115°–125° for ITO with CNT.

Table. Comparison of refractive properties of ITO modifications for p-polarization

Parameter	ITO modification		
	ITO	ITO with CNT	ITO with CNT and SEW
Parameters of extrema at α = 77°: λ (nm) / R_p (%)			
Maximum 1	358.3 nm / 20.3%	348.5 nm / 14.2%	330.6 nm / 13.2%
Minimum 1	437.3 nm / 13.9%	390.9 nm / 6.8%	387.2 nm / 6.1%
Maximum 2	593.3 nm / 22.2%	463.3 nm / 18.1%	535.7 nm / 16.7%
Minimum 2	The data are not applicable for the specified conditions	590.6 nm / 8.6%	The data are not applicable for the specified conditions
Maximum 3	The data are not applicable for the specified conditions	832.9 nm / 16.9%	The data are not applicable for the specified conditions
Average R_p value (%) in the visible range (400–750 nm) at different α			
α = 65°	18.5%	12.8%	13.5%
α = 71°	6.4%	3.4%	4.7%
α = 77°	1.8%	0.8%	1.2%

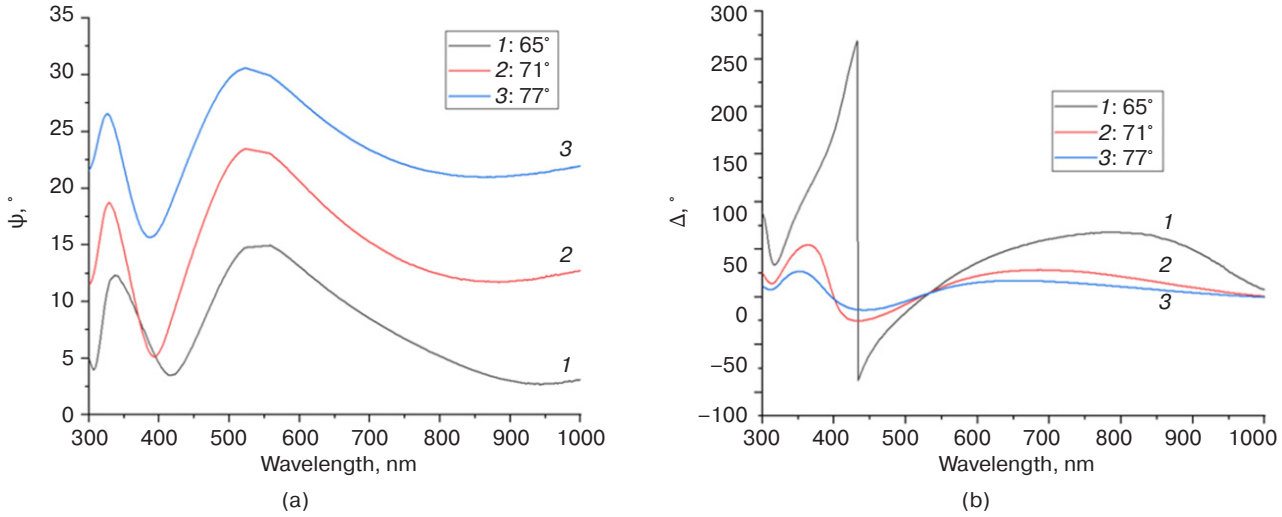

(a) (b)

Fig. 9. Spectral dependencies of ellipsometric parameters ψ (a) and Δ (b) of ITO films with CNT on K8 crown substrate after SEW-treatment in the range of 300–1000 nm at different angles of incidence: 65°, 71°, and 77°

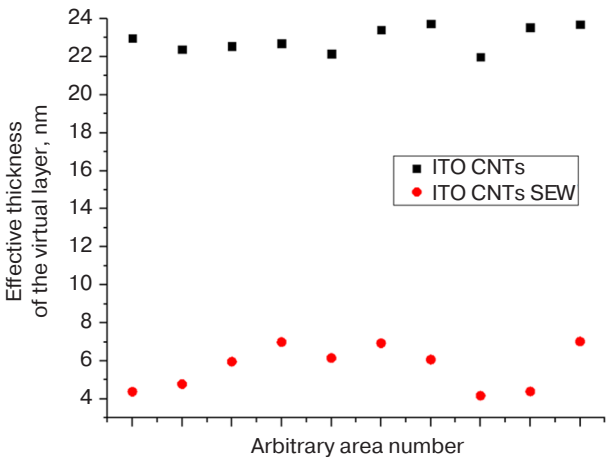

Fig. 10. Effective CNT layer thickness before and after SEW treatment determined on the basis of the ellipsometry method

Thus, the data on the change of refractive properties presented in the current study, as well as in a separate study devoted to wetting mechanisms during laser ablation and SEW treatment [26], indicate that a part of CNT clusters remains on the ITO surface at the selected mode of SEW treatment, resulting in thickness variation. Additional information on the effect of SEW treatment can be obtained from atomic force microscopy.

Figure 11a shows the surface profile of CNT on the ITO film prior to SEW treatment. The mean-square roughness *Sq* is 41.2 nm, while the maximum height h_{max} and h_{min} depth with respect to the zero-level line are 573.9 and −65.9 nm, respectively. It should be understood that CNTs are deposited in clusters of different height and density; thus, the parameters *Sq*, h_{max}, h_{min} are different in different surface areas. However, a tendency of decreasing roughness can be distinguished in SEW

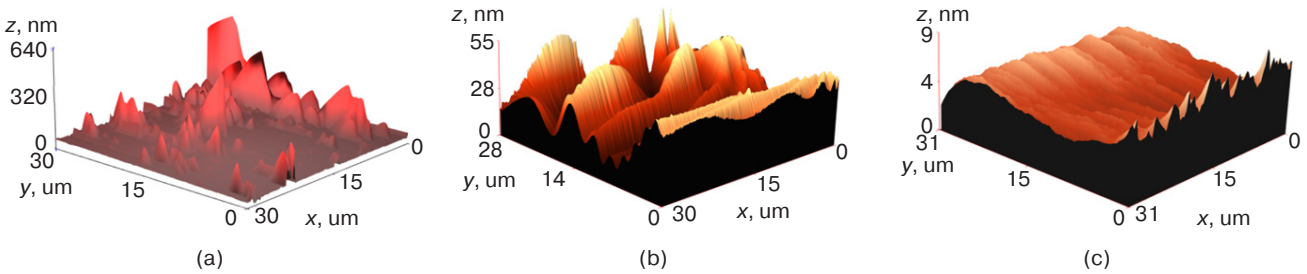

Fig. 11. Effect of SEW treatment on the surface of CNT deposited on ITO films: (a) before treatment; (b) SEW treatment of the region with high density of CNT deposition; (c) SEW treatment of the region with low density of CNT deposition

treatment. The case shown in Fig. 11b corresponds to SEW treatment of CNT with high deposition density: here, depressions are observed, which can be related both to a thinning of CNT clusters and a partial removal of ITO material. A decrease in the *Sq* value to 11.0 nm at h_{max} = 32.2 nm and h_{min} = −22.9 nm is observed. In cases where the density of deposited CNT is lower, such as when single tubes of small size are deposited on the ITO surface, the SEW treats the ITO surface to a greater extent than CNT (Fig. 11c). These regions are even smoother: *Sq* = 0.9 nm, h_{max} = 32.2 nm, h_{min} = −22.9 nm.

When evaluating the effect of SEW on the CNT layer thickness, the atomic force microscopy method has a limitation related to the ratio between the sizes of probes (up to 3–5 μm) and scanned objects (diameter of single CNT 1–2 nm). It is also necessary to take into account the adhesion of probes to CNT clusters, which causes additional measurement errors. Therefore, the noncontact ellipsometry method is preferable for solving this task.

CONCLUSIONS

Two important scientific and methodological results were obtained in the course of the performed research:

1. The effective thickness h_{eff} of the layer of laser-deposited single-walled carbon nanotubes on the ITO surface was determined. At the value of the control field strength of 100 V/cm in the process of CNT deposition on the ITO surface by the optical nondestructive method, the values of h_{eff} were determined to be in the range of 22–24 nm. Knowing the numerical value of this parameter allows us to perform calculations more efficiently in the development of electro-optical devices.
2. It is shown that the effective thickness of the CNT layer on the ITO surface can be precisely reduced by SEW treatment. For example, in the current study, it was possible to reduce h_{eff} from 22–24 nm to 4–8 nm. This is an important application of nanoplasmonics in the context of ITO surface treatment, since the accuracy of direct laser ablation directly depends on the **technical parameters** of the optical system (beam divergence, focal length, diameter, scanner pitch, etc.), while the accuracy of SEW treatment is determined by the **material properties** (n, μ, ω_{pl}).

The performed research and analysis contribute to the expansion of the material science database of photonics systems and functional materials of optoelectronics.

Thus, the effective thickness of the CNT layer on the ITO surface can be both increased (by means of additional oriented deposition) and precisely reduced by means of SEW treatment. This makes it possible to rearrange the interference peaks of thin films based on ITO with CNT as a means of optimizing the parameters of electro-optical devices with respect to the required spectral range. At the same time, the useful properties of CNT are preserved, i.e., an increase in coating strength, rearrangement of wetting mechanisms and optical luminescence, as well as an increase in electrical conductivity.

Aknowledgments

This research was partially supported by the Russian Science Foundation, grant No. 24-23-00021.

Authors' contributions

A.S. Toikka—setting up and conducting experiments, interpretation of the results, conceptualizing, drafting and editing the article.

N.V. Kamanina—interpretation of the results, conceptualization, editing the article.

REFERENCES

1. Kim H., Gilmore C.M., Piquie A., Horwitz J.S., Mattoussi H., Murata H., Kafafi Z.H., Chrisey D.B. Electrical, optical, and structural properties of indium–tin–oxide thin films for organic light-emitting devices. *J. Appl. Phys*. 1999;86(11): 6451–6461. https://doi.org/10.1063/1.371708
2. Adurodija F.O., Izumi H., Ishihara T., Yoshioka H., Motoyama M., Murai K. Influence of substrate temperature on the properties of indium oxide thin films. *J. Vac. Sci. Technol. A*. 2000;18:814–818. https://doi.org/10.1116/1.582260
3. Zhang K., Zhu F., Huan C.H.A., Wee T.S. Effect of hydrogen partial pressure on optoelectronic properties of indium tin oxide thin films deposited by radio frequency magnetron sputtering method. *J. Appl. Phys*. 1999:86(2):974–980. https://doi.org/10.1063/1.370834
4. Kerkache L., Layadi A., Mosser A. Effect of oxygen partial pressure on the structural and optical properties of dc sputtered ITO thin films. *J. Alloys Compd*. 2019;18(1):46–50. https://doi.org/10.1016/j.jallcom.2009.06.103
5. Kim J.-H., Lee J.-H., Heo Y.-W., Kim J.-J., Park J.-O. Effects of oxygen partial pressure on the preferential orientation and surface morphology of ITO films grown by RF magnetron sputtering. *J. Electroceram*. 2009;23:169–174. https://doi.org/10.1007/s10832-007-9351-8
6. Yang S., Sun B., Liu Y., Zhu J., Song J., Hao Z., Zeng X., Zhao X., Shu Y., Chen J., Yi J., He J. Effect of ITO target crystallinity on the properties of sputtering deposited ITO films. *Ceram. Int*. 2020;46(5):6342–6350. https://doi.org/10.1016/j.ceramint.2019.11.110
7. Chen Y., Du C., Sun L., Fu T., Zhang R., Rong W., Cao S., Li X., Shen H., Shi D. Improved optical properties of perovskite solar cells by introducing Ag nanoparticles and ITO AR layers. *Sci. Rep*. 2011;11:14550 https://doi.org/10.1038/s41598-021-93914-1
8. Chu F., Wang D., Liu C., Li L., Wang W.H. Multi-View 2D/3D Switchable Display with Cylindrical Liquid Crystal Lens Array. *Crystals*. 2021;11(6):715. https://doi.org/10.3390/cryst11060715
9. Rasheed M., Barille R. Optical constants of DC sputtering derived ITO, TiO_2 and TiO_2:Nb thin films characterized by spectrophotometry and spectroscopic ellipsometry for optoelectronic devices. *J. Non. Cryst. Solids*. 2017;476:1–14. https://doi.org/10.1016/j.jnoncrysol.2017.04.027
10. Losego M.D., Efremenko A.Y., Rhodes C.L., Cerruti M.G., Franzen S., Maria J.P. Conductive oxide thin films: Model systems for understanding and controlling surface plasmon resonance. *J. Appl. Phys*. 2009;106(2):024903. https://doi.org/10.1063/1.3174440
11. Amin R., Maiti R., Gui Y., Suer C., Miscuglio M., Heidari E., Khurgin J.B., Chen R.T., Dalir H., Sorger V.J. Heterogeneously integrated ITO plasmonic Mach–Zehnder interferometric modulator on SOI. *Sci. Rep.* 2021;11:1287. https://doi.org/10.1038/s41598-020-80381-3
12. Dong W.J., Yu H.K., Lee J.L. Abnormal dewetting of Ag layer on three-dimensional ITO branches to form spatial plasmonic nanoparticles for organic solar cells. *Sci. Rep.* 2020;10:12819. https://doi.org/10.1038/s41598-020-69320-4
13. Liu C., Wang J., Wang F., Su W., Yang L., Lv J., Fu G., Li X., Liu Q., Sun T., Chu P.K. Surface plasmon resonance (SPR) infrared sensor based on D-shape photonic crystal fibers with ITO coatings. *Opt. Commun.* 2020;464:125496. https://doi.org/10.1016/j.optcom.2020.125496
14. El Nahrawy A.M., Abou Hammad A.B., Youssef A.M., Mansour A.M., Othman A.M. Thermal, dielectric and antimicrobial properties of polystyrene-assisted/ITO:Cu nanocomposites. *Appl. Phys. A.* 2019;125:46. https://doi.org/10.1007/s00339-018-2351-5
15. Mei F., Huang J., Yuan T., Li R. Effect of cerium doping on the microstructure and photoelectric properties of Ce-doped ITO films. *Appl. Surf. Sci.* 2020;509:144810. https://doi.org/10.1016/j.apsusc.2019.144810
16. Taha H., Jiang Z.T., Yin C.Y., Henry D.J., Zhao X., Trotter G., Amri A. A Novel Approach for Fabricating Transparent and Conducting SWCNTs/ITO Thin Films for Optoelectronic Applications. *J. Phys. Chem. C.* 2018;122(5):3014–3027. https://doi.org/10.1021/acs.jpcc.7b10977
17. Kamanina N.V., Vasil'ev P.Ya., Studeonov V.I., Usanov Yu.E. Strengthening transparent conductive coatings and "soft" materials of the IR range when nanotechnologies are used. *J. Opt. Technol.* 2008;75(1):67–68. https://doi.org/10.1364/JOT.75.000067
[Original Russian Text: Kamanina N.V., Vasil'ev P.Ya., Studeonov V.I., Usanov Yu.E. Strengthening transparent conductive coatings and "soft" materials of the IR range when nanotechnologies are used. *Opticheskii zhurnal*. 2008;75(1):83–84 (in Russ.).]
18. Kamanina N., Toikka A., Gladysheva I. ITO conducting coatings properties improvement via nanotechnology approach. *Nano Express*. 2021;2(1):010006. https://doi.org/10.1088/2632-959X/abd90c
19. Kamanina N., Toikka A., Valeev B., Kvashnin D. Carbon Nanotubes Use for the Semiconductors ZnSe and ZnS Material Surface Modification via the Laser-Oriented Deposition Technique. *C – Journal of Carbon Research*. 2021;7(4):84. https://doi.org/10.3390/c7040084
20. Garcia-Caurel E., De Martino A., Gaston J.P., Yan L. Application of Spectroscopic Ellipsometry and Mueller Ellipsometry to Optical Characterization. *Appl. Spectroscopy*. 2013;67(1):1–21. https://doi.org/10.1366/12-06883
21. Fujiwara H. *Spectroscopic Ellipsometry.* The Atrium, Chichester, West Sussex, England: John Wiley & Songs; 2007. 369 p.
22. König T.A.F., Ledin P.A., Kerszulis J., Mahmoud M.A., El-Sayed M.A., Reynolds J.R., Tsukruk V.V. Electrically Tunable Plasmonic Behavior of Nanocube–Polymer Nanomaterials Induced by a Redox-Active Electrochromic Polymer. *ACS Nano*. 2014;8(6):6182–6192. https://doi.org/10.1021/nn501601e

23. Ermolaev G.A., Tsapenko A.P., Volkov V.S., Anisimov A.S., Gladush Y.G., Nasibulin A.G. Express determination of thickness and dielectric function of single-walled carbon nanotube films. *Appl. Phys. Lett*. 2020;116:231103. https://doi.org/10.1063/5.0012933
24. Toikka A.S., Fedorova L.O., Kamanina N.V. Influence of laser-deposited carbon-containing nanoparticles on the orienting properties of indium-tin-oxide-based conducting layers for liquid crystal devices. *J. Opt. Technol.* 2024;91(1):55–60. https://doi.org/10.1364/JOT.91.000055
[Original Russian Text: Toikka A.S., Fedorova L.O., Kamanina N.V. Influence of laser-deposited carbon-containing nanoparticles on the orienting properties of indium-tin-oxide-based conducting layers for liquid crystal devices. *Opticheskii zhurnal*. 2024;91(1):91–100 (in Russ.).]
25. Bonch-Bruevich A.M., Libenson M.N., Makin V.S., Trubaev V.V. Surface electromagnetic waves in optics. *Opt. Eng*. 1992;31(4):718–730. https://www.doi.org/10.1117/12.56133
26. Toikka A.S., Kamanina N.V. Formation of the anisotropic ITO-based orienting layers for the liquid crystal devices. *St. Petersburg State Polytechnical University Journal. Physics and Mathematics*. 2023;16(3.2):244–248. https://www.doi.org/10.18721/JPM.163.242

About the authors

Andrei S. Toikka, Postgraduate Student, Photonics Department, St. Petersburg Electrotechnical University "LETI" (5, ul. Professora Popova, St. Petersburg, 197022 Russia); Junior Researcher, Advanced Development Division, B.P. Konstantinov Petersburg Nuclear Physics Institute, National Research Center "Kurchatov Institute" (1, Orlova Roshcha, Gatchina, Leningradskaya oblast, 188300 Russia). E-mail: astoikka.nano@gmail.com. Scopus Author ID 57216272706, RSCI SPIN-code 1261-2571, https://orcid.org/0000-0002-8694-8497

Natalia V. Kamanina, Dr. Sci. (Phys.-Math.), Head of the Laboratory of Photophysics of Nanostructured Materials and Devices, Research and Production Corporation "S.I. Vavilov State Optical Institute" (36, Babushkina ul., St. Petersburg, 192171 Russia); Head of the Laboratory of Photophysics of Media with Nanoobjects, Vavilov State Optical Institute (5, Kadetskaya Liniya V.O., St. Petersburg, 199053 Russia), Professor, Photonics Department, St. Petersburg Electrotechnical University "LETI" (5, ul. Professora Popova, St. Petersburg, 197022 Russia); Lead Researcher of Advanced Development Division, B.P. Konstantinov Petersburg Nuclear Physics Institute, National Research Center "Kurchatov Institute" (1, Orlova Roshcha, Gatchina, Leningradskaya oblast, 188300 Russia). E-mail: nvkamanina@mail.ru. Scopus Author ID 55980751700, RSCI SPIN-code 1231-5045, https://orcid.org/0000-0002-2903-2685

Об авторах

Тойкка Андрей Сергеевич, аспирант, кафедра фотоники, ФГАОУ ВО «Санкт-Петербургский государственный электротехнический университет «ЛЭТИ» им. В.И. Ульянова (Ленина) (СПбГЭТУ «ЛЭТИ») (197022, Россия, Санкт-Петербург, ул. Профессора Попова, д. 5); младший научный сотрудник, отдел перспективных разработок, ФГБУ «Петербургский институт ядерной физики им. Б.П. Константинова «ПИЯФ» Национального исследовательского центра «Курчатовский институт» (188300, Россия, Ленинградская обл., Гатчина, Орлова роща, д. 1). E-mail: astoikka.nano@gmail.com. Scopus Author ID 57216272706, SPIN-код РИНЦ 1261-2571, https://orcid.org/0000-0002-8694-8497

Каманина Наталия Владимировна, д.ф.-м.н., заведующая отделом фотофизики наноструктурированных материалов и устройств, АО «Научно-производственное объединение «Государственный оптический институт им. С.И. Вавилова» (192171, Россия, Санкт-Петербург, ул. Бабушкина, д. 36); заведующая лаборатории фотофизики сред с нанообъектами, АО «Государственный оптический институт им. С.И. Вавилова» (199053, Россия, Санкт-Петербург, Кадетская линия В.О., д. 5); профессор, кафедра фотоники, ФГАОУ ВО «Санкт-Петербургский государственный электротехнический университет «ЛЭТИ» им. В.И. Ульянова (Ленина) (СПбГЭТУ «ЛЭТИ») (197022, Россия, Санкт-Петербург, ул. Профессора Попова, д. 5); ведущий научный сотрудник, отдел перспективных разработок, ФГБУ «Петербургский институт ядерной физики им. Б.П. Константинова «ПИЯФ» Национального исследовательского центра «Курчатовский институт» (188300, Россия, Ленинградская обл., Гатчина, Орлова роща, д. 1). E-mail: nvkamanina@mail.ru. Scopus Author ID 55980751700, SPIN-код РИНЦ 1231-5045, https://orcid.org/0000-0002-2903-2685

Translated from Russian into English by Lyudmila O. Bychkova
Edited for English language and spelling by Thomas A. Beavitt